TOWARDS AUTOMATED DETERMINATION OF ORBIT MANEUVERS FOR GNSS SATELLITES

Gottlob Gienger[*] and Filipe Lopes Pereira[†]

ESOC's navigation support office routinely performs precise orbit determination for GPS, GLONASS and Galileo navigation satellites. The orbit determination process including maneuvering satellites, using >500 station passes per satellite per day requires: (i) Automated search of station passes for orbit maneuvers (ii) Precise location of their start and end times (iii) Automated Delta-V estimation. Impulsive and non-impulsive maneuver models were tested on operational tracking data sets with Mathematica. The best performing algorithms were implemented into ESOC's Navigation Package for Earth Orbiting Satellites. Tests conducted on GPS orbit maneuvers 2011/2012 show very good agreement with the values published by Center for Orbit Determination in Europe. Delta-V maneuvers can now be identified within a few hours after their completion and duly considered in IGS products.

INTRODUCTION

As analysis centre of the International GNSS Service (IGS), ESOC's navigation support office routinely performs precise orbit determination for GPS, GLONASS and Galileo navigation satellites. Precise location of orbit maneuver intervals as well as estimation of the ΔV is indispensable for precise orbit determination.

This task is characterized by the following facts:

- No spacecraft telemetry is available at ESOC.
- The Center for Orbit Determination in Europe (CODE) provides maneuver magnitudes and mid-times in their final product summary reports, but these have a latency of 1-2 weeks (Reference 1). Being the only Analysis Center providing orbit solutions for maneuvering satellites at the moment, it is the solution adopted by IGS in their Rapid and Final products, and our reference.
- Typically, for each GNSS satellite, there are >300 stations and >500 station passes per day to process, which prevents routine visual inspection of plotted range data for signatures of a ΔV.

---

[*] Flight Dynamics engineer, Research and Technology Management Office (HSO-GX), ESA/ESOC, Robert-Bosch-Str. 5, 64293 Darmstadt, Germany
[†] Aerospace engineer, GMV S.A. - on contract at the European Space Agency, Navigation Support Office (HSO-GN), ESA/ESOC, Robert-Bosch-Str. 5, 64293 Darmstadt, Germany

Therefore ESOC's navigation support office took steps towards an automated determination of ΔV maneuvers:

- Automated search for station passes where a ΔV occurs
- Locate start and end times of the ΔV as precisely as possible from all maneuver passes
- Perform precise orbit determination on the arcs before and after the ΔV
- Estimate the ΔV-vector.

A two-step approach was chosen:

Step 1: Identify the best suitable algorithms

To exploit various approaches, we developed Mathematica notebooks to

- Import observation files, containing time, station, ionosphere-free phase, ionosphere-free range, simulated range without maneuver, elevation
- Prepare data file for analysis
- Find the passes containing ΔV by binning the differences between ionosphere-free phase [range resp.] signal and simulated range and the separating signature of a maneuver from measurement noise.
- Plot data for maneuver passes
- Prepare data sets for fitting
- Fit maneuver models to data. The following maneuver models were fitted against data:

  - Impulsive velocity change, integrated for range
  - Ditto, concatenated with post-maneuver sinusoids
  - Rectangular acceleration profile, integrated for velocity, integrated for range
  - Ditto, concatenated with post-maneuver sinusoids.
- Compare quality of fits. In general, the last model gave the best results.

Step 2: Implement the best algorithms into operational environment

The best performing algorithms were implemented into NAPEOS, the Navigation Package for Earth Orbiting Satellites (FORTRAN 95):

- Use ionosphere-free carrier phase residuals, giving precise one-way ranging information, as input data.
- Computed observations based on the most recent orbit prediction before the maneuver takes place
- Selection of valid passes taking into account minimum elevation angle, pass duration and cycle slips. Consistency checks and outlier rejection.
- Use trust-region algorithm for nonlinear model fit, estimating 4 parameters: Maneuver start & end times, magnitude and period of post-maneuver sinusoid.
- Besides the usual parameters for precise orbit determination, radial, along and cross track maneuver errors are estimated, with loose constraints.

Tests conducted on all GPS orbit maneuvers from Jan. 2011 to Feb. 2012 show very good agreement with the values published by CODE. The success of this method is very much dependent on tracking data quality and requires a global network of GNSS receivers able to track "unhealthy" satellites.

BACKGROUND ON GNSS SATELLITE ORBIT MANOEUVRES

Both gravitational forces (Earth oblateness and higher spherical harmonics, luni-solar perturbations) and non-gravitational forces (mainly solar radiation pressure, Earth albedo, satellite infrared re-emission, antenna radiation, relativistic effects) continuously disturb the circular MEO orbits of the GNSS satellites. In the event of a satellite failure, the Master Control Station can reposition satellites to maintain an optimal GNSS constellation. Therefore the GNSS operations control centers assign slots for orbit maintenance or repositioning satellites.

The frequency of station-keeping maneuvers depends to a large extent on the orbit characteristics, and in particular on the commensurability of the orbit period with the Earth's rotation period In the case of GPS there is a 2:1 relationship and under these circumstances, the satellite motion will be in resonance with geopotential terms. The actual magnitude of the resonance perturbations will depend strongly on the orbit inclination and on the relative position of the orbital nodes w.r.t. the Earth. At a sub-optimal orbit inclination of 55°, GPS satellites will be subject to a daily drift rate in the semi-major axis of up to 7 m/day (reference 5), in case the resonant oscillation is at the unstable equilibrium point.

At a slightly lower orbit, GLONASS satellites have an orbital period of only 11h15 and therefore, they are not subject to resonance perturbations. This explains why GLONASS orbit-maintenance maneuvers are not done so frequently.

In this work, we do not consider the orbit maneuvers required in LEOP after separation from launcher to position the GNSS satellites into their operational orbits and the de-orbiting maneuvers at the end of their operational lifetime.

Facts about GNSS satellite propulsion systems

Since the relevant information about the propulsion systems of the generations of GNSS satellites is dispersed over hundreds of sources, we have summarized it in Table 1.

Table 1. GNSS satellite propulsion systems.

	Manu-facturer	Satel-lite bus	Reference or URL	Launch mass	Propulsion	Acceleration per thruster
GPS Block II	Rock-well International	-	ftp://tycho.usno.navy.mil/pub/gps/gpsb2.txt http://www.aerojet.com http://www.astronautix.com/engines/mr103.htm	1660 kg	Hydrazine Attitude control MR-103 1.12 N	13.4 mm/s^2
GPS Block IIA	Rock-well International	-	http://en.wikipedia.org/wiki/GPS_Block_IIA#Block_IIA_series	1816 kg	Orbit control MR-50 22.2 N	12.2 mm/s^2
GPS Block IIR	Lockheed-Martin	AS 4000 was used for all 21 GPS IIR satellites	http://www.astronautix.com/craft/as4000.htm	2032 kg	Hydrazine MR-103 16×1.12 N	0.6 mm/s^2
GPS Block IIR-M				2060 kg		0.5 mm/s^2

GPS Block IIF	Boeing	GPS IIF	http://en.wikipedia.org/wiki/GPS_IIF_SV-1	1630 kg		0.7 mm/s^2
GLON ASS 1st genera-tion	Resh-netev (for-merly NPO of Applied Mechan-ics)		(Reference 2) (Reference 3) section 10.5.4 http://www.astronautix.com/craft/glonass.htm Fakel experimental design bureau http://www.fakel-russia.com/	1250 kg	Hydrazine Fakel Attitude K50-10.4 1 N Orbit 2×5 N (2×500 g)	4 mm/s^2
GLON ASS S/N 20 L ff.				1400 kg		3.6 mm/s^2
GLON ASS-M	Reshet-nev		http://www.tsenki.com/en/launch_services/help_information/launch/2011/?EID=87008	1415 kg (1480 kg)		3.5 mm/s^2
GLON ASS-K	Reshet-nev	Express 1000	http://www.tsenki.com/en/launch_services/help_information/launch/2011/?EID=86266	935 kg		5.4 mm/s^2
GIOVE A	Surrey Satellite Tech-nology Ltd	Mini-Sat-400	(Reference 4) Starsem GIOVE-A launch kit http://www.starsem.com/news/kits.htm http://www.astronautix.com/craft/minat400.htm http://www.sstl.co.uk/Downloads/Datasheets/Subsys-datasheets/Butane-Propulsion-System	602 kg	Butane 10×50 mN	0.08 mm/s^2
GIOVE B	Galileo Indus-tries		(Reference 4) Starsem GIOVE-B launch kit http://www.starsem.com/news/kits.htm http://www.giove.esa.int/page_index.php?menu=103&page_id=36	501 kg	Hydrazine 8×1 N	2 mm/s^2
Galileo IOV 1-4	EADS Astrium		(Reference 4) http://cs.astrium.eads.net/sp/spacecraft-propulsion/showcase/galileo-esa.html	700 kg	Hydrazine 8×1 N	1.4 mm/s^2

Typical size and duration of orbit control maneuvers

The observed sizes of ΔV maneuvers range from a few cm/s up to 2-3 m/s; see Table 5. Dividing the magnitude of the ΔV by the acceleration of the orbit thrusters in Table 1, one expects pure maneuver durations (with continuous firing, without operational overhead) of 1 minute up to several hours. If orbit control is performed in pulsed mode firing with an on/off duty cycle for example of dc=0.1, then the maneuver duration gets prolonged by a factor 1/dc=10.

Orbit maneuver information distributed by navigation centers

The handling of ΔV maneuvers by AIUB CODE is described in (Reference 1): "Starting with beginning of 2004, satellite maneuvers are monitored, maneuver epoch and velocity change are determined and orbits before and after the event are provided in the precise orbit files (making use of the maneuver flag available in SP3c.) Maneuver parameters are documented in CODE's

weekly analysis summaries beginning with GPS week 1252." Figure 4 therein shows how the mean epoch and time interval of the velocity change is assigned.

Table 2. Orbit maneuver information by navigation centers.

Satellites	Reference or URL	Recent orbit maneuvers
GPS	Notice Advisory to NAVSTAR Users (NANU) http://www.navcen.uscg.gov/?pageName=selectNanuByNumber	In 2011, there were 106 NANUs issued. 23 of them were of type FCSTDV=Forecast Delta-V 23 ΔVs per year
		From 1.1.-29.2.2012, there were 16 NANUs issued, 3 of them of type FCSTDV 3 ΔV per 60 days projected 18 ΔVs per year
GLONASS	http://www.glonass-ianc.rsa.ru/en/GLONASS/	No indication of ΔVs performed
GPS	AIUB CODE (Reference 1) CODE final GNSS products, available at	Processed information from GPS NANUs
GLONASS	ftp://ftp.unibe.ch/aiub/CODE/yyyy CODwwww7.SUM.Z Weekly GNSS analysis summary files contain ΔV information for GPS and GLONASS, e.g. COD16307.SUM `Day 095: PRN G18 repositioned at approx. 17:51:24 GPST Estimated components of velocity change in or- bital frame:    -0.1 mm/sec (radial)  -137.6 mm/sec (along track)   -2.3 mm/sec (out of plane)`	Only one in 2011 Day 119: PRN R07
		None 2012-01-01 until 2012-02-15
GIOVE-A	Notice Advisory to GIOVE Users (NAGU) http://www.giove.esa.int/nagu.php?menu=12	Only one on 2009-01-30
GIOVE-B	Apply filter: Category=ANY Type=Orbit maneuver.	None
Galileo IOV	-	-

PROBLEM ANALYSIS WITH MATHEMATICA

Several versions of Mathematica notebooks (Reference 6) were developed to test various approaches of automated ΔV detection and mathematical or physical models for the maneuvers and to validate their robustness and performance on operational GNSS observation data. Mathematica input/output is indicated by Courier new font, e.g. `deltat = 30 Second`.

Test data sets

As test data sets, NAPEOS[*] derived observation data in ASCII format were used, which tabulate for one day for one GNSS satellite with 30 s sampling frequency the following quantities, typically >200,000 records. As representative example, we use file OBS_G18_11095 for GPS satellite PRN[†]=G18 (SVN[‡]=54), date 2011/04/05=2011-095:

```
Date-Time         Station  Iono-free         Iono-free         Simulated        Elevation
                           Phase[km]         Range[km]         range[km]        [°]

2011/04/05-       ABMF     24767.818702619   24767.910073818   24767.90860868   12.216
15:08:15.000

2011/04/05-       ABMF     24757.833715496   24757.921823544   24757.922307193  12.312
15:08:45.000
```

Important note on column 3 "ionosphere free phase": The overall phase measurement will contain an unknown number of carrier-cycles (ambiguity) which will remain constant as long as the receiver remains locked on the signal[§]. Figure 1(a) shows an example.

Column 5 "Simulated range" is calculated based on the predicted orbit. The essential signature of a maneuver is a gradual increase in difference between col. 3 and col. 5 and between col. 4 and col. 5. After the end of the maneuver, a periodic oscillation with one orbital period persists, the difference between the old and new Kepler orbit. It is essential that (i) the predicted orbit is precise enough, (ii) the predicted orbit excludes the ΔV (e.g. CODE rapid not valid); otherwise just a transient is visible in the differences instead of a permanent deviation.

Preprocessing

Since the Mathematica function `AbsoluteTime["string"]` e.g. on a Sun Ultra 45 running Solaris is too slow for such large amounts of data, a Mathematica utility reads in a selected NAPEOS observation file, converts the first date-time column into integer seconds once, appends the results as last column (col. 7) and stores the augmented table back on disk as two-dimensional Mathematica list. These augmented files are read in subsequently for data manipulations, numeric calculations and date-time plots.

Prepare data file for analysis

This comprises the following sub-steps:

1. Read two-dimensional list into variable `rangedatat`
2. Define a reasonable gap size `gaps = 1800 Second` and split into separate tables for each station pass:
   ```
   rangedatas = Split[rangedatat, -#1[[7]] + #2[[7]] < gaps && #1[[2]]
   == #2[[2]] &]
   ```

---

[*] See http://dgn7.esoc.esa.int/tools/napeos-navigation-package-for-earth-observation-satellites/ for an overview and next section
[†] Pseudo-Random Noise code
[‡] Space Vehicle Number
[§] Explanation for the initial phase values offsets: The carrier "beat" phase observable is the phase of the signal remaining after the internal oscillated frequency generated in the receiver is differenced from the incoming carrier signal, which can have an arbitrary value. Once the receiver locks on to a particular satellite it keeps a running cycle count based on this Doppler frequency shifts present on the L1 and L2 carrier frequencies.

Typically, there are 500-600 station passes per day, duration varying between isolated single samples and 9 h.

3. Calculate the difference between col. 3 (iono-free phase) and col. 5 (simulated range):

```
phasediff0 = Table[Max[Abs[rangedatas[[i, All, 3]] - rangedatas[[i,
All, 5]]]], {i, Length[rangedatas]}]
```

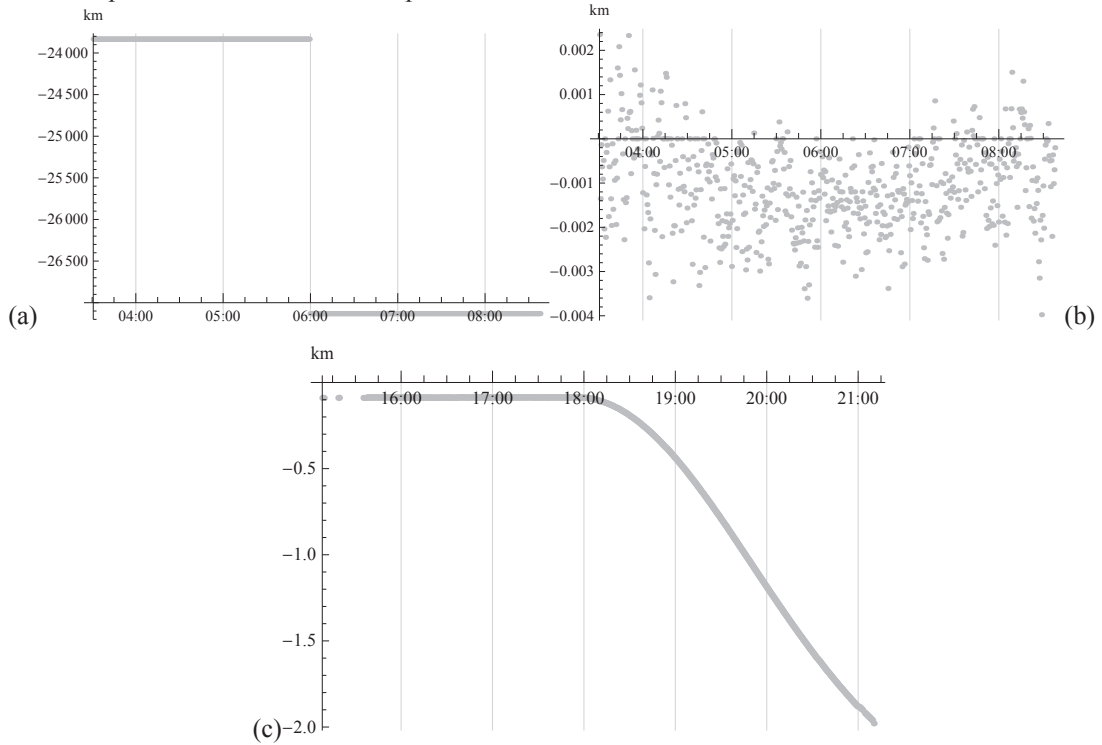Inspection reveals at least four possibilities:

(a) (b)

(c)

Figure 1. Possible signatures in `phasediff0`: (a) Large initial phase offset, followed by a cycle slip at 06:00, (b) measurement noise, (c) orbit maneuver.
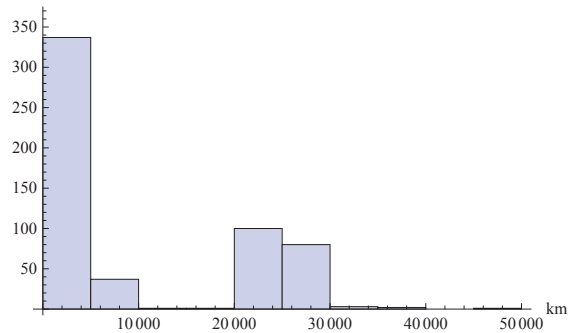
Figure 2. `Histogram[phasediff0].`

137

4. Remove initial offsets: Subtract the difference between the first element of col. 3 (iono-free phase) and col. 5 (simulated range) of `rangedatas`.
5. Create modified list

```
phasediff = Table[Max[Abs[rangedatas[[i, All, 3]] - rangedatas[[i,
All, 5]]]], {i, Length[rangedatas]}]
```
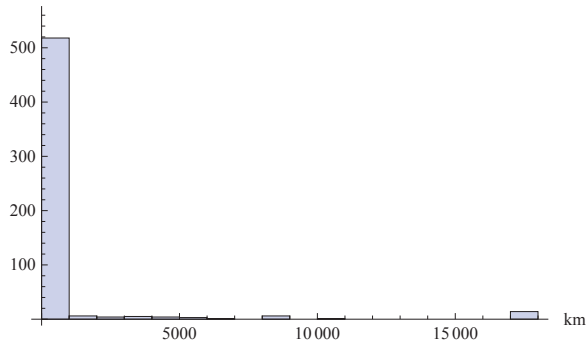

Figure 3. `Histogram[phasediff].`

This clearly concentrates the histogram onto the first bin.

Finding the passes containing a ΔV

1. Find sets of passes containing the maneuver, applying three criteria
   1.1. Based on maneuver times reported by AIUB CODE or manual input: Defines set `manpass0`
   1.2. Based on phase differences: This is done via binning `phasediff` with successively smaller bin sizes, until a zero bin followed by a secondary positive bin count is found. This is a candidate for a maneuver pass.
      1.2.1.Initialize `BinCounts (Histogram)` parameters
        `{xmax = 2.0, dx = 0.1} (*km*)`
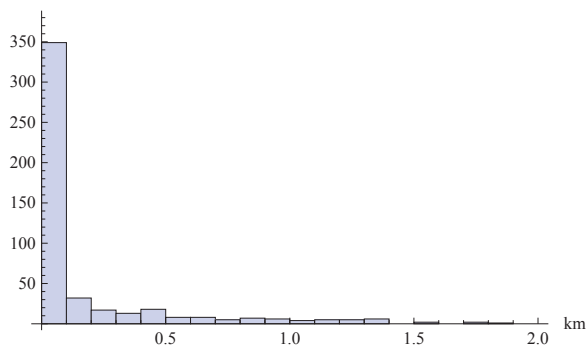   1.2.2.Halve the interval and bin size, until there is a zero bin count followed by a positive bin count.

Figure 4. `Histogram[phasediff, {0, xmax, dx}].`

```
BinCounts[phasediff, {0, xmax, dx}]
{349,32,17,13,18,8,8,5,7,6,4,5,5,6,0,2,0,2,1,0}
```

138

1.2.3. Take the first zero bin count as limit

```
limit1 = dx (first0bin[phasediff, xmax, dx] - 1)
```

1.2.4. Extract the pass numbers exceeding the limit

```
manpass1 = Position[Positive[phasediff - limit1], True]
```

  1.3. Based on range differences: Applying the same steps as for `phasediff` gives set `man-pass2`

2. Pick out the passes containing the maneuver:

```
manpass = Intersection[manpass0, manpass1, manpass2]
```

3. Sort passes containing the maneuver e.g. by duration, this gives a short list like

```
{{365,"RCMV","2011/04/05-13:15:45.000","2011/04/05-20:42:45.000"},
{240,"LMMF","2011/04/05-15:04:15.000","2011/04/05-21:32:45.000"},
{232,"KOUR","2011/04/05-16:04:15.000","2011/04/05-22:08:15.000"},
{1,"ABMF","2011/04/05-15:08:15.000","2011/04/05-21:10:15.000"},
{261,"MAS1","2011/04/05-16:18:45.000","2011/04/05-20:46:45.000"},
{153,"GMAS","2011/04/05-16:18:45.000","2011/04/05-20:46:45.000"}}
```

4. Extract the full maneuver datasets

```
mandatas = rangedatas[[sortmanpass]]; Map[Dimensions, mandatas]
{{895, 7}, {778, 7}, {729, 7}, {671, 7}, {537, 7}, {537, 7}}
```

5. User to select one of the maneuver passes: E.g. to choose the "KOUR" pass, which has the longest coverage post maneuver, `select=3`.

Prepare data sets for fitting

1. Start and end time of pass: `{tpass0,tpass1}`
2. Define time scale relative to start of pass to avoid large numbers of order 10^9 s

```
times = Partition[mandatas[[select, All, 7]] - tpass0, 1]
```

3. Observed minus predicted range | range rate | range rate rate data

```
drange = 1000 Transpose
[{mandatas[[select, All, 3]] - mandatas[[select, All, 5]],
mandatas[[select, All, 4]] - mandatas[[select, All, 5]]}]; (*Meter*)
drangerate = Differences[drange]/deltat[[1]]; (*Meter/Second*)
drangeraterate = Differences[drangerate]/deltat[[1]];
(*Meter/Second^2*)
```

4. Create datasets for fitting range, velocity and acceleration models

```
rangedata = Join[times, drange, 2];
veldata = Join[MovingAverage[times, 2], drangerate, 2];
accdata = Join[MovingAverage[times, 3], drangeraterate, 2];
```

Maneuver models

Acceleration, velocity and range were modeled for impulsive and non-impulsive maneuvers. Their behavior is shown in the results of fits (color lines).

Table 3. Impulsive and non-impulsive maneuver models.

Impulsive ΔV	`velimp[deltav_,timpulse_,t_]:=deltav Piece-`
	`wise[{{1,t>=timpulse}}]`
	`rangeimp[deltav_,timpulse_,t_]:=deltav Max[0,t-timpulse]`

Impulsive ΔV con-catenated with sinu-soids	`velimps[deltav_,timpulse_,period_,t_]:=deltav Piece-`
	`wise[{{Cos[2 Pi/period(t-timpulse)],t>=timpulse}}]`
	`rangeimps[deltav_,timpulse_,period_,t_]:=deltav period/(2 Pi)`
	`Piecewise[{{Sin[2 Pi/period (t-timpulse)],t>=timpulse}}]`

Rectangular acceleration profile	`accmodelv[deltav_,tstart_,tend_,t_]:=Piecewise[{{deltav/(tend-tstart),tstart<=t<=tend}}]`
	`velmodelv[deltav_,tstart_,tend_,t_]:=Piecewise[{{deltav/(tend-tstart)(t-tstart),tstart<=t<=tend},{deltav,tend <t}}]`
	`rangemodelv[deltav_,tstart_,tend_,t_]:=Piecewise[{{deltav/(tend-tstart)/2(t-tstart)^2,tstart<=t<=tend},{deltav/2(tend-tstart)+deltav (t-tend),t>tend}}]`

Rectangular acceleration profile concatenated with sinusoids	`accmodelvs[deltav_,tstart_,tend_,period_,t_]:=`
	`Piecewise[{{deltav/(tend-tstart),tstart<=t<=tend},{-2 Pi/period deltav Sin[2 Pi/period (t-tend)],t>tend}}]`
	`velmodelvs[deltav_,tstart_,tend_,period_,t_]:=`
	`Piecewise[{{deltav/(tend-tstart)(t-tstart),tstart<=t<=tend},{deltav Cos[2 Pi/period(t-tend)],tend<t}}]`
	`rangemodelvs[deltav_,tstart_,tend_,period_,t_]:=`
	`Piecewise[{{deltav/(tend-tstart)/2(t-tstart)^2,tstart<=t<=tend},{deltav/2(tend-tstart)+deltav period/(2 Pi) Sin[2 Pi/period (t-tend)],t>tend}}]`

Fitting maneuver models

1. Define suitable initial values
   1.1. Define coarse starting values
   ```
   {t0 = First[Flatten[times]], t1 = Last[Flatten[times]]}
   ```
   1.2. Select the first time where the range or velocity or acceleration deviates more than 6 standard deviations from flat
   ```
   outlier[values_?VectorQ, nsamples_?IntegerQ] :=
   Positive[Abs[values] - 6 StandardDeviation[values
   [[;; Min[nsamples, Length[values]]]]]]
   toutlier[times_?VectorQ, values_, nsamples_] :=
   Pick[times, outlier[values, nsamples]]
   toutlier1[times_, values_, nsamples_] := First[toutlier[times,
   values, nsamples]]
   tstart0 = Flatten[Table[toutlier1[Flatten[times], drange[[All,
   i]], 10], {i, 2}]]
   ```
   1.3. Initial value of Delta V including sign from range data
   ```
   deltav0 = (drange[[-1, All]] - drange[[1, All]])/(t1 - tstart0)
   (*Meter/Second*)
   ```
   1.4. Initial value for maneuver end time `tend0 = (tstart0 + t1)/2`

2. Fit impulsive Delta-V models (red) to data (grey), vertical gridline = `timpulse`
   ```
   Do [rangefit[i] = NonlinearModelFit[rangedata[[All, {1, i + 1}]]],
   rangeimp[deltav, timpulse, t], {{deltav, deltav0[[i]]}, {timpulse,
   tstart0[[i]]}}, t], {i, 2}]
   ```
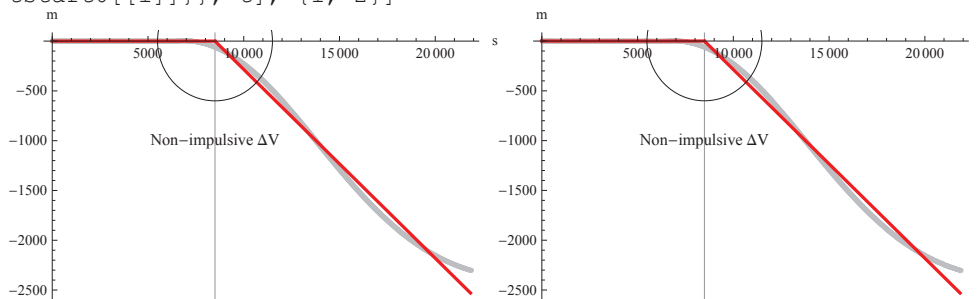
- Estimate of `timpulse` is reasonable
- Linear slope post maneuver cannot match sinusoidal data

```
Do [velfit[i] = NonlinearModelFit[veldata[[All, {1, i + 1}]],
velimp[deltav, timpulse, t], {{deltav, deltav0[[i]]}, {timpulse,
tstart0[[i]]}}, t], {i, 2}]
```
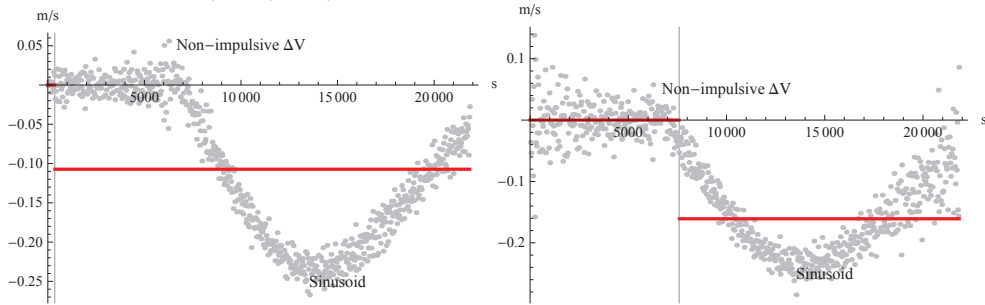

- Model `velimp` estimates `timpulse` too early; it should be at the midpoint of the slope
- Caused by sinusoidal tail of data after end of maneuver

3. Fit impulsive Delta-V concatenated with sinusoids (orange) to data (grey)

```
period0=43200 Second (* approximately 1 orbital period *)
Do [rangefit[i + 2] = NonlinearModelFit
[rangedata[[All, {1, i + 1}]], rangeimps[deltav, timpulse, period,
t], {{deltav, deltav0[[i]]}, {timpulse, tstart0[[i]]},
{period, period0[[1]]}}, t], {i, 2}]
```


- Estimate of `timpulse` is reasonable

```
Do [velfit[i + 2] = NonlinearModelFit
[veldata[[All, {1, i + 1}]], velimps[deltav, timpulse, period, t],
{{deltav, deltav0[[i]]}, {timpulse, tstart0[[i]]},
{period, period0[[1]]}}, t], {i, 2}]
```
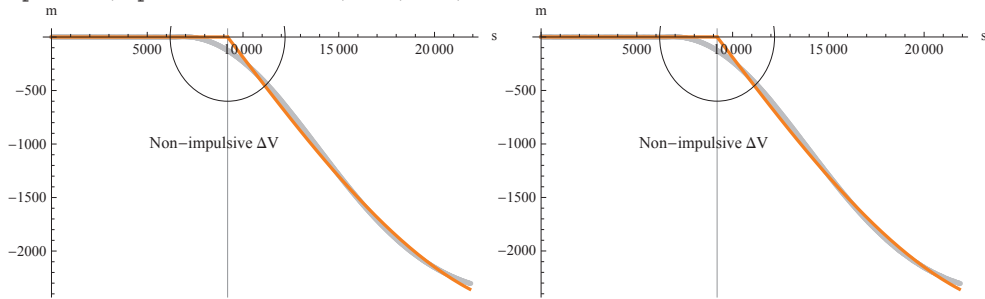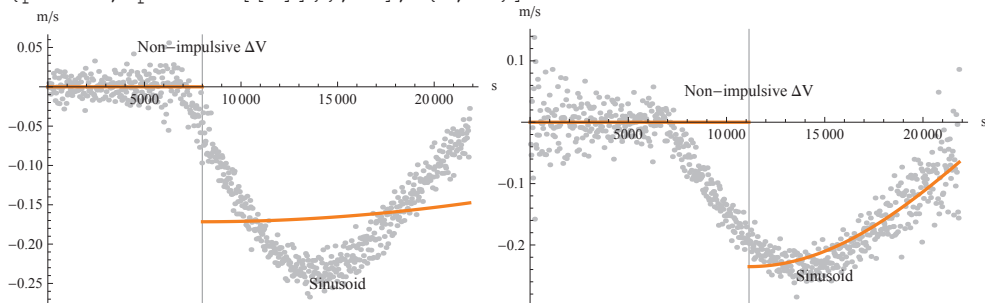

- Estimate of `timpulse` is reasonable
- Period estimate of post maneuver sinusoid wrong
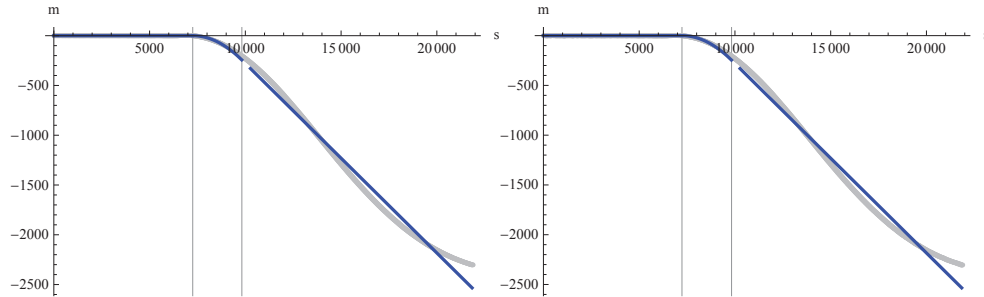
141

4. Fit rectangular acceleration profile functions (blue) to data (grey), vertical gridlines at tstart, tend

```
Do [rangefit[i + 4] = NonlinearModelFit
[rangedata[[All, {1, i + 1}]]],rangemodelv[deltav, tstart, tend, t],
{{deltav, deltav0[[i]]}, {tstart, tstart0[[i]]}, {tend, tend0[[i]]}},
t], {i, 2}];
```


- rangemodelv may give a poor fit to tstart and tend
- The transition from parabola to linear drift at tend is hard to locate with function fit
- Therefore the ΔV size may be overestimated
- The straight lines post maneuver obviously cannot match the sinusoidal data behavior

```
Do[velfit[i + 4] = NonlinearModelFit
[veldata[[All, {1, i + 1}]]], velmodelv[deltav, tstart, tend, t],
{{deltav, deltav0[[i]]}, {tstart, tstart0[[i]]}, {tend, tend0[[i]]}},
t], {i, 2}];
```
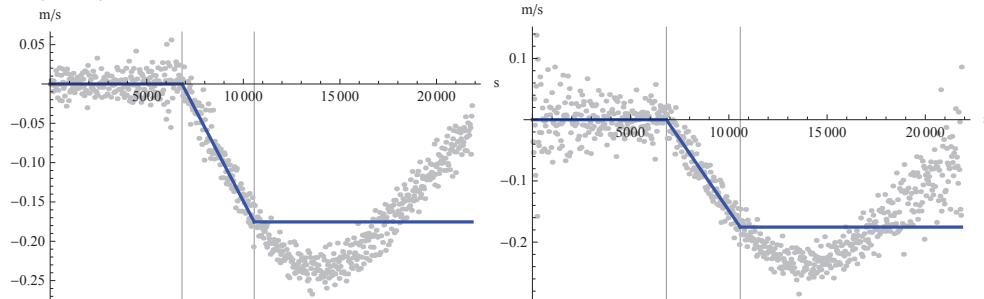

- velmodelv gives a reasonable estimate to tstart and tend
- The flat lines post maneuver obviously cannot match the sinusoidal data behavior

```
Do[accfit[i] = NonlinearModelFit
[accdata[[All, {1, i + 1}]]], accmodelv[deltav, tstart, tend, t],
{{deltav, deltav0[[i]]}, {tstart, tstart0[[i]]}, {tend, tend0[[i]]}},
t], {i, 2}]
```


- The datasets are mostly noise

142

- Estimates of `tstart` and `tend` are erratic.

5. Fit rectangular acceleration profile with sinusoids to data

```
Do[rangefit[i + 6] = NonlinearModelFit
[rangedata[[All, {1, i + 1}]], rangemodelvs[deltav, tstart, tend, pe-
riod, t], {{deltav, deltav0[[i]]}, {tstart, tstart0[[i]]}, {tend,
tend0[[i]]}, {period, period0[[1]]}}, t], {i, 2}]
```
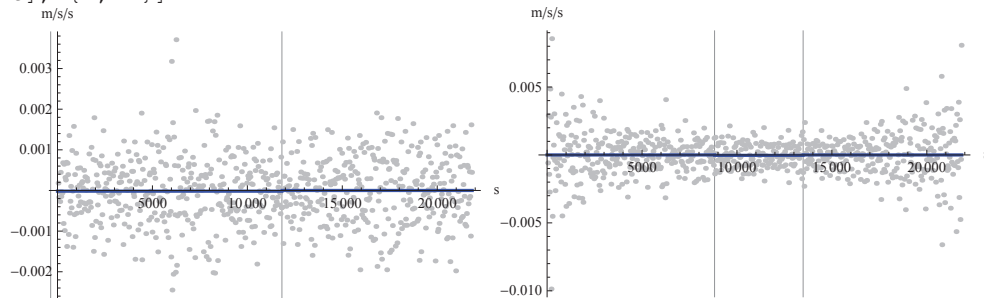

- Perfect fit!

```
Do[velfit[i + 6] = NonlinearModelFit
[veldata[[All, {1, i + 1}]], velmodelvs[deltav, tstart, tend, period,
t], {{deltav, deltav0[[i]]}, {tstart, tstart0[[i]]}, {tend,
tend0[[i]]}, {period, period0[[1]]}}, t], {i, 2}];
```


- Some noise, but perfect fit!

```
Do[accfit[i + 2] = NonlinearModelFit
[accdata[[All, {1, i + 1}]], accmodelvs[deltav, tstart, tend, period,
t], {{deltav, deltav0[[i]]}, {tstart, tstart0[[i]]}, {tend,
tend0[[i]]}, {period, period0[[1]]}}, t], {i, 2}];
```
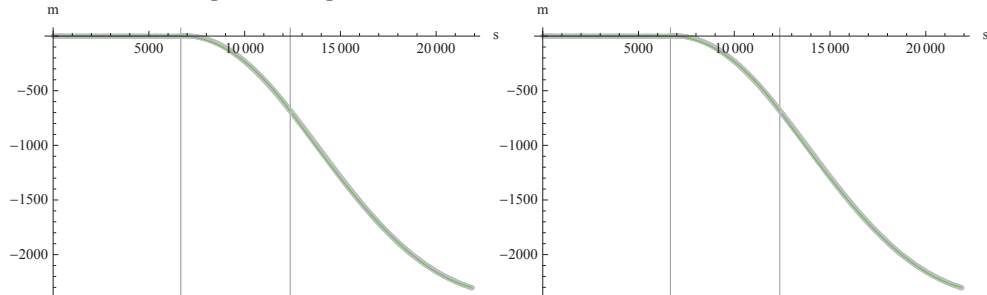

- The datasets are mostly noise
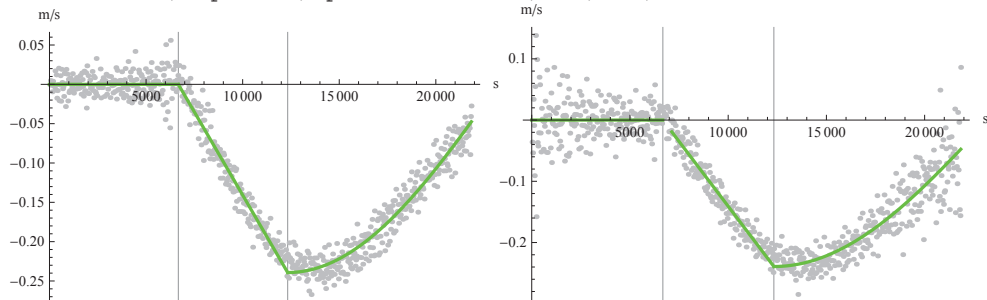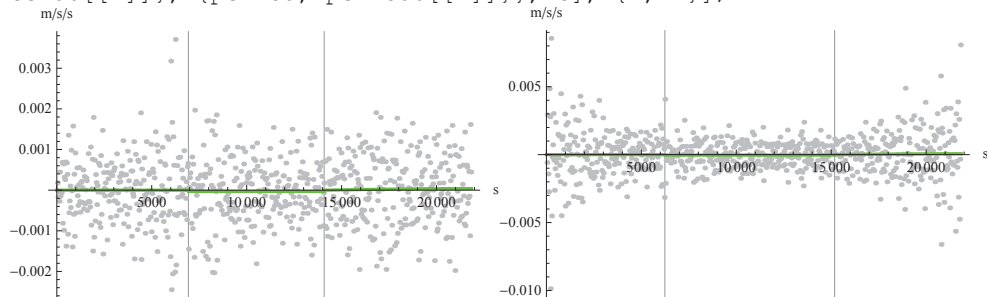- Estimates of `tstart` and `tend` are erratic.

143

Compare quality of fits

This is done using the `"ParameterTable"` property of the various fitted models[*]:

1. Simple impulsive models

```
MatrixForm[Join[Table[rangefit[i]["ParameterTable"],{i,2}],
Table[velfit[i]["ParameterTable"],{i,2}]]]
```

	Estimate	Standard Error	t Statistic	P−Value
deltav	−0.189622	0.000748294	−253.406	$1.944193511850885 \times 10^{-711}$
timpulse	8498.97	30.4367	279.235	$9.03954992044693 \times 10^{-742}$
	Estimate	Standard Error	t Statistic	P−Value
deltav	−0.189512	0.000745743	−254.125	$2.535356446231209 \times 10^{-712}$
timpulse	8489.04	30.3503	279.702	$2.709786793646431 \times 10^{-742}$
	Estimate	Standard Error	t Statistic	P−Value
deltav	−0.107235	0.00336907	−31.8292	7.42419×10^{-140}
timpulse	360.	0.	∞	$0. \times 10^{-308}$
	Estimate	Standard Error	t Statistic	P−Value
deltav	−0.160809	0.00255437	−62.9543	2.61376×10^{-296}
timpulse	7590.	0.	∞	$0. \times 10^{-308}$

- `rangemodelv` gives rough estimates of `deltav`, `timpulse`
- `velmodelv` gives poor estimates of `deltav`, wrong estimate of `timpulse`

2. Impulsive models with sinusoids

	Estimate	Standard Error	t Statistic	P−Value
deltav	−0.235349	0.0011071	−212.582	$4.98069235539 \times 10^{-656}$
timpulse	9196.25	18.6184	493.935	$8.30830360413 \times 10^{-920}$
period	68736.2	795.813	86.3722	$3.65779434595 \times 10^{-384}$
	Estimate	Standard Error	t Statistic	P−Value
deltav	−0.23531	0.00111189	−211.631	$1.228217221099 \times 10^{-654}$
timpulse	9190.58	18.7188	490.982	$6.37587033455 \times 10^{-918}$
period	68773.	799.653	86.0035	$6.19835521730 \times 10^{-383}$
	Estimate	Standard Error	t Statistic	P−Value
deltav	−0.171582	0.00644001	−26.6431	1.42368×10^{-109}
timpulse	7995.	8444.42	0.94678	0.344067
period	162385.	98105.8	1.6552	0.0983162
	Estimate	Standard Error	t Statistic	P−Value
deltav	−0.235287	0.00978955	−24.0345	2.4793×10^{-94}
timpulse	11145.	1301.66	8.56217	6.60053×10^{-17}
period	52077.7	6964.27	7.47784	2.18654×10^{-13}

3. Simple rectangular acceleration profiles

---

[*] Mathematica formats the table entries slightly different for the first pair, second pair (and third pair)

	Estimate	Standard Error	t Statistic	P-Value
deltav	-0.190396	0.000832041	-228.83	$6.56304928055 \times 10^{-679}$
tstart	7252.97	192.362	37.7048	3.7838×10^{-173}
tend	9818.32	219.37	44.7569	6.0063×10^{-211}

	Estimate	Standard Error	t Statistic	P-Value
deltav	-0.190346	0.00083197	-228.789	$7.45751192458 \times 10^{-679}$
tstart	7233.81	191.487	37.777	1.50688×10^{-173}
tend	9823.35	218.636	44.9301	7.64536×10^{-212}

	Estimate	Standard Error	t Statistic	P-Value
deltav	-0.175374	0.00217997	-80.448	$1.419960520381713 \times 10^{-363}$
tstart	6826.76	162.595	41.9862	2.70926×10^{-196}
tend	10562.6	168.427	62.713	4.58405×10^{-295}

	Estimate	Standard Error	t Statistic	P-Value
deltav	-0.175409	0.00249964	-70.1734	$1.886785646777220 \times 10^{-325}$
tstart	6819.57	184.15	37.0327	2.5114×10^{-169}
tend	10579.	191.687	55.1892	8.54007×10^{-262}

	Estimate	Standard Error	t Statistic	P-Value
deltav	-0.209456	0.498896	-0.419838	0.674728
tstart	-360.	8.57936×10^{-6}	-4.19612×10^{7}	$5.69789838278 \times 10^{-4486}$
tend	11820.	8.57936×10^{-6}	1.37772×10^{9}	$8.78359378985 \times 10^{-5584}$

	Estimate	Standard Error	t Statistic	P-Value
deltav	-0.148676	0.573717	-0.259145	0.795597
tstart	8820.	0.0000182846	4.82372×10^{8}	$8.47890885493 \times 10^{-5254}$
tend	13485.	0.0000182846	7.37505×10^{8}	$2.725883140726 \times 10^{-5387}$

- `rangemodelv` and `velmodelv` give reasonable accuracies on `deltav`, `tstart`, `tend`

- `accmodelv` cannot estimate any parameter correctly! Therefore drop the last two fits.

4. Rectangular acceleration profiles with sinusoids

	Estimate	Standard Error	t Statistic	P-Value
deltav	-0.240187	0.000136657	-1757.59	$5.526991876722169 \times 10^{-1318}$
tstart	6682.34	7.44823	897.171	$2.334025355859108 \times 10^{-1106}$
tend	12373.	10.6022	1167.02	$4.247886593639567 \times 10^{-1189}$
period	-42988.2	98.1195	-438.121	$3.943639329956864 \times 10^{-881}$

	Estimate	Standard Error	t Statistic	P-Value
deltav	-0.240085	0.000136708	-1756.18	$9.86850285662466 \times 10^{-1318}$
tstart	6665.41	7.44574	895.198	$1.150091670422834 \times 10^{-1105}$
tend	12377.8	10.6131	1166.28	$6.734920506727024 \times 10^{-1189}$
period	42963.4	98.2488	437.291	$1.550332455813603 \times 10^{-880}$

	Estimate	Standard Error	t Statistic	P-Value
deltav	-0.239265	0.00117704	-203.277	$8.20240989824 \times 10^{-641}$
tstart	6669.72	52.4489	127.166	$1.803704221779 \times 10^{-497}$
tend	12331.4	50.5781	243.809	$3.736401752148 \times 10^{-697}$
period	43589.9	422.401	103.196	$3.023006261266 \times 10^{-435}$

	Estimate	Standard Error	t Statistic	P-Value
deltav	-0.239196	0.00216633	-110.415	$3.070570945329 \times 10^{-455}$
tstart	6675.	97.2019	68.6715	$2.804388808313 \times 10^{-319}$
tend	12325.5	92.9983	132.535	$6.14854358202 \times 10^{-510}$
period	43630.1	777.549	56.1123	7.68139×10^{-266}

	Estimate	Standard Error	t Statistic	P-Value
deltav	-0.2133	3.63939	-0.0586086	0.95328
tstart	6930.	134514.	0.0515188	0.958926
tend	14080.8	17770.1	0.79239	0.428393
period	33467.1	396399.	0.0844277	0.93274

	Estimate	Standard Error	t Statistic	P-Value
deltav	-0.305617	6.39096	-0.0478203	0.961873
tstart	6240.12	200658.	0.0310983	0.9752
tend	15180.	18713.3	0.811187	0.417525
period	28743.	417262.	0.0688847	0.9451

- rangemodelvs gives the best accuracy on deltav, tstart, tend, period
- velmodelvs gives less accuracy
- accmodelvs cannot estimate any parameter correctly! Therefore drop the last two fits

5. From the two fits using rangemodelvs and two fits using velmodelvs, select the one with smallest total of relative parameter errors. This finally gives the following results for the three longest passes:

Table 4. Best fit maneuver parameters and confidence intervals for GPS PRN G18 on 2011-095.

Fit parameter		RMCV	LMMF	KOUR
ΔV size	Lower limit	-0.205233 m/s	-0.226689 m/s	-0.240456 m/s
	Best fit	-0.204726 m/s	-0.226343 m/s	-0.240187 m/s
	Upper limit	-0.204219 m/s	-0.225998 m/s	-0.239919 m/s
tstart	Lower limit	16196.8 s 2011-095T17:45:41	10018.8 s 2011-095T17:51:13	6667.71 s 2011-095T17:55:22
	Best fit	16209.2 s 2011-09517:45:54	10033.1 s 2011-095T17:51:28	6682.34 s 2011-095T 17:55:37
	Upper limit	16221.6 s 2011-095T17:46:06	10047.4 s 2011-095T17:51:42	6696.96 s 2011-095T17:55:51
tend	Lower limit	21461.2 s 2011-095T19:13:26	15585.1 s 2011-095T19:24:00	12352.1 s 2011-095T19:30:07
	Best fit	21488.3 s 2011-095T19:13:53	15608.8 s 2011-095T19:24:23	12373.0 s 2011-095T19:30:27
	Upper limit	21515.4 s 2011-095T19:14:20	15632.4 s 2011-095T19:24:47	12393.8 s 2011-095T19:30:48
period	Lower limit	74218.9 s	45620.9 s	-43180.8 s
	Best fit	78254.6 s	45997.3 s	-42988.2 s
	Upper limit	82290.2 s	46373.8 s	-42795.6 s

Lessons learned from Mathematica implementation and test cases

1. The best estimation results are achieved with rectangular range profile combined with post maneuver sinusoids.
2. The estimated ΔV magnitudes for this maneuver are significantly larger than the impulsive ΔV magnitude given by AIUB CODE |ΔV|=0.13762 m/s in Table 2.
3. The maneuver start times agree reasonably within 10 min and with the AIUB CODE start time 17:51:24 GPST in Table 2.
4. The maneuver end times have a larger spread of ~ 17 min, because of short datasets post maneuver, esp. for the RMCV pass, which ends at 20:42 i.e. 75 to 90 min after the ΔV end.
5. The estimated confidence intervals of tstart and tend are unrealistically small compared to the spread of the estimates from different passes.
6. There is a large spread in the estimates of the period of the post maneuver sinusoids. Obvious reason is the short remaining time from end of ΔV to end of passes.

IMPLEMENTATION IN NAPEOS

NAPEOS (Navigation Package for Earth Orbiting Satellites) is a portable navigation software system for Earth Orbiting satellite missions, providing orbit determination/prediction, maneuver-planning and parameter estimation capabilities. It is able to process a wide variety of observation data including angles, range, range-rate, altimetry, satellite-to-satellite and Global Navigation

Satellite System data. In particular, the following tracking systems are supported: GNSS (GPS, GLONASS, Galileo), satellite laser ranging (SLR), DORIS, PRARE, MPTS, and LCT ranging.

NAPEOS is compliant with IERS 2003 Conventions and supports within ESOC all the activities in the International GNSS Service (IGS), International DORIS Service (IDS), International Laser Ranging Service (ILRS) and other international scientific communities.

Since the success of satellite maneuver detection depends, to a large extent, on the quality and availability of tracking data, the IGS station network was used in this analysis. This network consists of more than 300 globally distributed stations, equipped with high-end geodetic receivers. A growing number of these receivers is now tracking unhealthy satellites.

Maneuver Detection and Estimation Steps

The first step is to produce a valid a priori orbit. The process is based on the broadcast navigation messages collected from the CDDIS server or alternatively from the available tracking stations. Then the broadcast ephemerides are checked for consistency. Together with the satellite health flag information this provides an indication that a maneuver took place. In this case, two distinct state vectors are written to characterize the orbit before and after the event.

The second step is to detect the exact maneuver time, based on the best method as per the Mathematica analysis (rectangular range profile combined with post maneuver sinusoids). The implementation uses the Intel Math Kernel Library (Reference 8) for non-linear least squares estimation and the estimated parameters are the maneuver start and end times, the magnitude and the post-maneuver sinusoids. A-priori values are taken from iono-free pseudo-range (PR) residuals and residual differences:

- Maneuver start time defined when PR residual exceeds the detection limit (100m)
- Period of post-maneuver sinusoid taken as 43200 sec (orbit period)
- Maneuver magnitude (ΔV) defined has the residual at the point of maximum residual difference divided by the time since the maneuver start.
- Maneuver end time defined by the equation:

$$Maneuver_{end} = Maneuver_{start} + \frac{\Delta V}{Max.\,Acc} \quad , \quad Max.\,Acc\,(\text{Table}1) \tag{1}$$

If the pass is long enough and no cycle slips are detected, iono-free phase residuals are generated and stored. The a-priori values and the observation arrays are then used by the DTRNLS_POWELL (Intel MKL) routine which solves the non-linear least squares problem, using the trust-region algorithm. According to the Mathematica analysis the function used is the following (`rangemodelvs`):

$$Function(\Delta V, t_{start}, t_{end}, T) = \begin{cases} \dfrac{\Delta V \cdot (t - t_{start})^2}{2 \cdot (t_{end} - t_{start})}, & t_{start} \leq t \leq t_{end} \\[4mm] \dfrac{\Delta V \cdot (t_{end} - t_{start})}{2} + \dfrac{\Delta V \cdot T \cdot \sin\left(\dfrac{2\pi \cdot (t_{end} - t_{start})}{T}\right)}{2\pi}, & t > t_{end} \end{cases} \tag{2}$$

We further specified the maximum number of iterations (100) and the values for stop tests *eps(1-5)* = $1.0 \cdot 10^{-5}$. The algorithm informs about the status of task completion and the convergence of the process can be assessed.

147

$$\Delta k < eps(1) \qquad\qquad A - \text{Jacobi Matrix}$$
$$\|F(x)\| < eps(2) \qquad\qquad \Delta k - \text{Trust Region Area}$$
$$\|A(x)_{ij}\| < eps(3) \qquad\qquad F(x) - \text{Functional Value} \qquad (3)$$
$$\|s\| < eps(4) \qquad\qquad s - \text{Trial step}$$
$$\|F(x)\| - \|F(x) - A(x)s\| < eps(5)$$

The third step is to perform a first preliminary orbit estimation, by using Pseudo-range observations alone with the maneuver and the a priori orbit information obtained in the previous steps. This generates an orbit with accuracy in the meter level.

A further step of data cleaning is done, before the orbit estimation with pseudo-range and phase observations is attempted. The parameters estimated are the following:

- Satellite state vector
- CODE parameters of the solar radiation pressure model ($D0, Y0, B0, Bc, Bs$)
- Maneuver errors (radial, cross-track, along-track)
- CPR (Cycle Per Revolution) - To compensate for model imperfections ($A0, As, Ac$)

Figure 5 shows the resulting orbit accuracy, when compared with the IGS rapid product, based on the CODE solution.

Finally, we attempt to fix phase ambiguities on double differenced observations and estimate the final orbit including the maneuver. Given presence of discontinuities and the inherent inaccuracies in the maneuver start and end times, we were not able to see an improvement with respect to the float ambiguity solution.
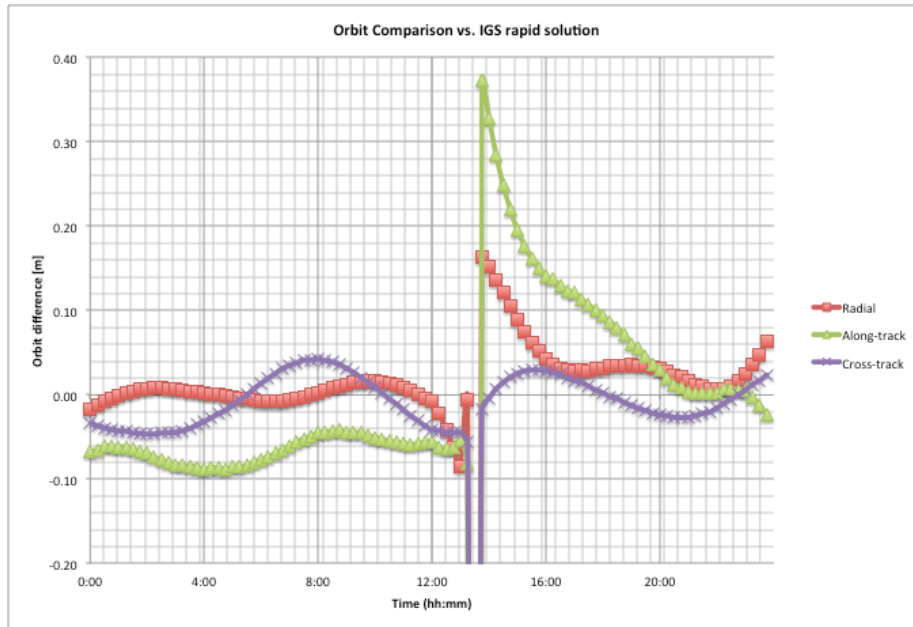

Figure 5. Comparison of NAPEOS orbit vs. IGS rapid for GPS satellite PRN 14.
Maneuver estimated at 2012-02-07T13:31:53 GPST (DOY 038).

TEST RESULTS

In order to validate the suggested maneuver detection method, we processed the last 20 GPS maneuver cases in NAPEOS and present the results in Table 5. The corresponding CODE solution as per the CODE weekly reports are shown for comparison. Maneuver start times, which constitute the most important parameter, are in good agreement: $Median_{NAPEOS-CODE} = 6\min 7\sec$

Table 5. Maneuver detection results.

| PRN	SVN	Date (yyddd)	Time CODE	ΔV CODE	Time NAPEOS	ΔV NAPEOS	Block (Clock)	Slot
27	27	12053	01:04:07	173.3	01:13:42	330.6	IIA (Cs)	A6
14	41	12038	13:26:46	162	13:31:53	293.3	IIR (Rb)	F1
25	62	11349	17:11:25	179.7	17:11:18	285.6	IIF (Rb)	B2
30	35	11340	20:21:56	1383.8	20:19:09	2087.8	IIA (Rb)	B5
05	50	11336	05:17:44	183.6	05:26:46	327.8	IIR-M (Rb)	E3
20	51	11334	03:54:23	205.9	04:00:56	365.5	IIR (Rb)	E1
31	52	11327	05:00:35	188.5	05:09:01	346.2	IIR-M (Rb)	A2
32	23	11322	03:46:29	209.7	03:51:05	386.0	IIA (Rb)	E5
16	56	11263	11:54:36	272.7	12:01:45	496.9	IIR (Rb)	B1
13	43	11244	16:52:22	171.8	17:01:44	331.1	IIR (Rb)	F3
02	61	11243	00:40:51	183.0	00:47:18	307.9	IIR (Rb)	D1
08	38	11238	10:04:21	134.5	10:10:03	252.7	IIA (Cs)	A3
06	36	11235	05:51:39	56.6	06:28:45	110.1	IIA (Rb)	C6
17	53	11223	20:21:12	173.1	20:31:14	331.7	IIR-M (Rb)	C4
24	24	11215	12:51:00	197.7	12:56:48	347.3	IIA (Cs)	D5
23	60	11125	17:46:09	164.3	17:44:21	265.5	IIR (Rb)	F4
11	46	11123	19:41:14	122.6	19:46:41	194.5	IIR (Rb)	D5
29	57	11111	09:23:05	203.4	09:31:24	381.3	IIR-M (Rb)	C1
18	54	11095	17:51:24	137.6	17:49:49	194.4	IIR (Rb)	E4
21	45	11046	13:48:12	155.2	13:50:12	251.6	IIR (Rb)	D3
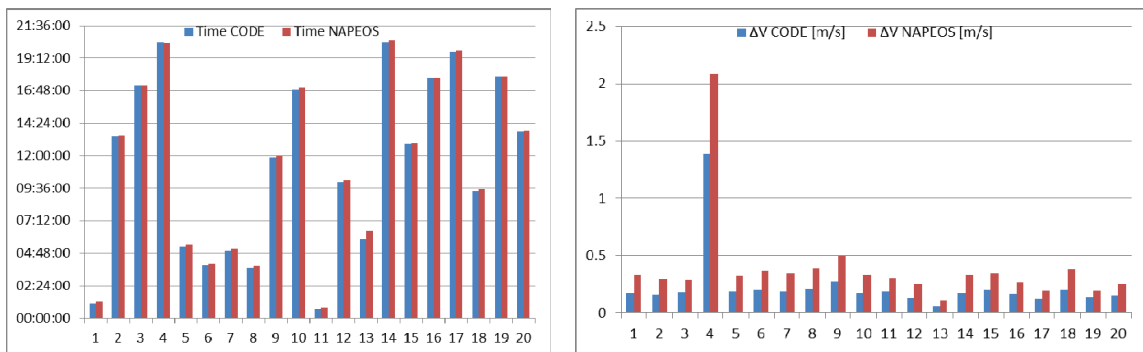
Figure 6. Comparison of GPS maneuvers 2011/2012 CODE vs. NAPEOS.

149

CONCLUSIONS, FURTHER STEPS

We have developed tools to automatically filter out maneuver passes from phase and range observation files and have successfully implemented the concept in the operational environment for testing.

Impulsive maneuver models give poor estimates of ΔV size and maneuver time. Integrated rectangular acceleration profiles give reasonable estimates of ΔV size, maneuver start and end times, esp. when combined with post maneuver sinusoids. It is relatively simple to detect the start of a maneuver and to locate it to the accuracy of a few minutes. It is more difficult to detect the physical end of the maneuver, using non-impulsive maneuver models and even more difficult to locate the end precisely. This is caused by the fact that the simulated range data are synchronized with ionosphere-free phase and range data at the start of the pass.

The current method looks promising for automated satellite maneuver detection and estimation in near real-time, especially for operations which demand the highest level of satellite availability. This method could potentially decrease the current satellite outage period after a maneuver takes place.

The estimation accuracy for the ΔV end times could be improved by creating a second set of simulated range data, synchronized with ionosphere-free phase and range data at the end of the passes. Then one can apply the same procedure as described above with time running from pass end to pass start and determine the end time of the maneuver with the same accuracy as the start of the maneuver by the forward procedure. This has to be tested and implemented.

So far, we have only used phase and range data. Fitting of the velocity models directly to Doppler data is expected to give more accurate parameter fits.

Further steps include validation against actual operation logs from GPS, GLONASS or Galileo Control Centers, and the assessment of new GNSS signals for maneuver detection, which could allow stronger and lower elevation tracking of maneuvering satellites, thus increasing the number of available tracking passes.

ACKNOWLEDGMENTS

REFERENCES

(Reference 1)   U. Hugentobler et al., *CODE IGS Analysis Center Technical Report 2003/2004*, Astronomical Institute University Bern.

(Reference 2)   Arkhipov, B. A., Vertakov, N. M., Didenko, B. E., & Niatin, A. G., *Development of Propulsion Units for Small Spacecraft*, ESA SP-465, 2001, p.763.

(Reference 3)   E. Kaplan (ed*.), Understanding GPS principles and applications*, Artech House, 1996.

(Reference 4)   *The First Galileo Satellites - Galileo In-Orbit Validation Element GIOVE*, ESA Brochure BR-251, 2nd imprint, August 2006.

(Reference 5)   U. Hugentobler, *Astrometry and satellite orbits: Theoretical consideration and typical applications*, Geodätisch-geophysikalische Arbeiten in der Schweiz, vol. 57, 1998.

(Reference 6)   *Wolfram Mathematica® 7*, ©Copyright 1988-2009 Wolfram Research, Inc.

(Reference 7)   T.A. Springer, *NAPEOS Mathematical Models and Algorithms*, DOPS-SYS-TN-0100-OPS-GN, issue 1.0, 2009.

(Reference 8)   *Intel Math Kernel Library 10.2.1*, Copyright © 1996-2009, Intel Corporation.